Title: Regional shape differentiation of the vertebral column shape in felids: a study of three-dimensional shape trajectories

Short-running tittle: 3D vertebral shape trajectories

Authors: Marcela Randau[1*], Andrew R. Cuff[1,2], John R. Hutchinson[2,1], Stephanie E. Pierce[3,2], Anjali Goswami[1,4]

Affiliation:

[1]Department of Genetics, Evolution and Environment, University College London, United Kingdom

[2]Department of Comparative Biomedical Sciences and Structure & Motion Laboratory, The Royal Veterinary College, United Kingdom

[3]Department of Organismic and Evolutionary Biology and Museum of Comparative Zoology, Harvard University, USA

[4]Department of Earth Sciences, University College London, United Kingdom

*corresponding author: m.randau@ucl.ac.uk

Acknowledgements

We thank the two peer reviewers for their excellent, constructive criticisms of the first draft of this paper. For access to museum collections, we thank R. Portela Miguez and R. Sabin at the Natural History Museum, London; M. Lowe and R. Asher at the University Museum of Zoology, Cambridge; C. Lefèvre at the Muséum National d'Histoire Naturelle, Paris; J. Chupasko at the Harvard Museum of Natural History, Cambridge; E. Westwig at the American Museum of Natural History, New York; W. Stanley at the Field Museum of Natural History, Chicago; and D. Lunde at the Smithsonian National Museum of Natural History, Washington D.C. This work was supported by Leverhulme Trust grant RPG 2013-124 to AG and JRH. This research received support from the SYNTHESYS

project http://www.synthesys.info/ which is financed by European Community Research Infrastructure Action under the FP7 "Capacities" Program. The SYNTHESYS grant was awarded to MR.

Abstract:

Recent advances in geometric morphometrics provide improved techniques for extraction of biological information from shape and have greatly contributed to the study of ecomorphology and morphological evolution. However, the vertebral column remains an under-studied structure due in part to a concentration on skull and limb research, but most importantly because of the difficulties in analysing the shape of a structure composed of multiple articulating discrete units (i.e. vertebrae).

Here, we have applied a variety of geometric morphometric analyses to three-dimensional landmarks collected on 19 presacral vertebrae to investigate the influence of potential ecological and functional drivers, such as size, locomotion, and prey size specialisation, on regional morphology of the vertebral column in the mammalian family Felidae. In particular, we have here provided a novel application of a method – Phenotypic Trajectory Analysis (PTA) – that allows for shape analysis of a contiguous sequence of vertebrae as functionally linked osteological structures.

Our results showed that ecological factors influence the shape of the vertebral column heterogeneously and that distinct vertebral sections may be under different selection pressures. While anterior presacral vertebrae may either have evolved under stronger phylogenetic constraints or are ecologically conservative, posterior presacral vertebrae, specifically in the post-T10 region, show significant differentiation among ecomorphs. Additionally, our PTA results demonstrated that functional vertebral regions differ among felid ecomorphs mainly in the relative covariation of vertebral shape variables (i.e. direction of trajectories, rather than in trajectory size) and, therefore, that ecological divergence among felid species is reflected by morphological changes in vertebral column shape.

Keywords: geometric morphometrics, morphological evolution, regionalisation, phenotypic trajectory analysis, ecomorphology, axial skeleton

Introduction:

From species description to detailed studies of ecomorphology, analyses of form have long been used by researchers examining ecological and evolutionary trends in both living and fossil organisms (e.g. Dumont et al. 2015; Lauder 1995; Rudwick 2005; Davies et al. 2007; Gonyea 1978; Gould 1966; Benoit 2010; Boszczyk et al. 2001; Goswami et al. 2014; Goswami et al. 2012). The geometric morphometrics revolution has greatly improved the scientific capacity to extract detailed information from biological structures. Yet it has also been hindered by computation issues with statistical tests used and the constraints involved in analysing data that are dense (e.g. large numbers of landmarks) and multidimensional, with specimen:landmark ratios decreasing as a result of these new advances (Mitteroecker and Gunz 2009; Adams et al. 2013; Collyer et al. 2014; Adams 2014b; Cardini and Loy 2013). Newly developed software and methods are rapidly tackling these analytical power issues, with a plethora of recent papers describing and applying these approaches to diverse morphometric datasets (e.g. Adams and Collyer 2009; Adams 2014a; Adams et al. 2015; Collyer et al. 2014; Adams 2014b; Sheets and Zelditch 2013; Mitteroecker and Gunz 2009; Monteiro 2013; Polly et al. 2013; Mitteroecker et al. 2013; Klingenberg and Marugán-Lobón 2013).

Among morphological studies in the vertebrate literature, both those using geometric morphometrics (GMM) and studies using linear or cross-sectional measurements, there is a clear bias towards the morphology of the skull (e.g. Meachen-Samuels and Van Valkenburgh 2009a; Slater and Van Valkenburgh 2008; Fabre et al. 2014; Stayton 2005; Figueirido et al. 2010; Goswami and Polly 2010; Goswami 2006; Pierce et al. 2008, 2009; Piras et al. 2013; Drake and Klingenberg 2010; Foth et al. 2012; Meachen et al. 2014), followed by studies of the limbs (e.g. Bennett and Goswami 2011; Fabre et al. 2013; Bell et al. 2011; Alvarez et al. 2013; Martin-Serra et al. 2014; Adams and Nistri 2010; Walmsley et al. 2012; Zhang et al. 2012; Andersson and Werdelin 2003; Ercoli et al. 2012; Sears et al. 2013; Meachen-Samuels and Van Valkenburgh 2009b; Doube et al. 2009). The axial skeleton, in contrast, is comparatively underrepresented in the morphological literature, with the majority of

91 work on this structure taking a biomechanical or developmental perspective (e.g. Macpherson and
92 Fung 1998; Boszczyk et al. 2001; Long et al. 1997; Molnar et al. 2015; Smeathers 1981; Wellik 2007;
93 Gál 1993; Müller et al. 2010; Buchholtz et al. 2012; Galis et al. 2014; Schilling and Long 2014; Narita
94 and Kuratani 2005; Chen et al. 2005; Buchholtz et al. 2014; Breit and Künzel 2004; Chatzigianni and
95 Halazonetis 2009). Additionally, due to the difficulties in studying a structure that is composed of
96 discrete units, research on axial skeletal morphology has frequently focused on separate analyses of
97 individual vertebrae, with a few studies presenting intervertebral comparisons of individual
98 measurements or differential morphospace occupation of vertebral types, rather than combined
99 analysis of the full column (e.g. Alvarez et al. 2013; Jones 2015; Arnold et al. 2016; Manfreda et al.
100 2006; Buchholtz et al. 2014). Nevertheless, the limited morphometric studies of vertebral form have
101 demonstrated that ecological specialisations and developmental patterning are reflected in the
102 morphology of individual vertebrae, as well as along the entire spine (e.g. Jones and German 2014;
103 Pierce et al. 2011; Shapiro 2007; Ward and Mehta 2014; Head and Polly 2015; Randau et al. 2016;
104 Werneburg et al. 2015; Jones and Pierce 2015; Böhmer et al. 2015; Johnson et al. 1999; Chen et al.
105 2005). Indeed, many large clades, including the vast majority of placental mammals, do not display
106 meristic changes (i.e. variation in number) in the axial skeleton; therefore, adaptation of this
107 structure must happen through modifications of its shape (Müller et al. 2010; Narita and Kuratani
108 2005; Buchholtz 2014; Buchholtz et al. 2012).

109 Recently, we conducted a large-scale linear morphometric analysis of the felid (cats) presacral
110 vertebral column and found that this method was unable to strongly differentiate taxa based on
111 either prey size specialization or locomotor mode (Randau et al. 2016). For instance, there were few
112 statistical differences in vertebral profile plots (i.e. variation in linear measures along the column),
113 and a principal components analysis found a locomotory signal only in the lumbar region. These
114 results were surprising considering felid prey size specialization has been shown to correlate with
115 osteological measures of the skull and appendicular skeleton (Meachen-Samuels and Van
116 Valkenburgh 2009a, 2009b; Slater and Van Valkenburgh 2008) and similar linear morphometric

117 studies on other mammalian groups (e.g. pinnipeds, whales) have found the vertebral column to hold
118 a strong ecological signal (e.g. Pierce et al. 2011; Buchholtz 2001a, 2001b; Hua 2003; Finch and
119 Freedman 1986). As felids are a morphologically conservative group, with little variation in
120 musculoskeletal anatomy across the clade (Doube et al. 2009; Cuff et al. 2016b, 2016a; Day and
121 Jayne 2007), it remains uncertain whether the felid vertebral column holds little ecological signal or if
122 linear morphometric techniques are not powerful enough to discriminate more subtle variation in
123 vertebral form. To investigate this further, we extend our work by quantifying vertebral morphology
124 in felids using three-dimensional landmarks-based GMM, and include a novel application of
125 phenotypic trajectory analysis (Adams and Collyer 2009; Collyer and Adams 2013) to identify
126 ecological signal in serial structures. Three-dimensional (3D) landmarks are expected to provide
127 greater detail and biological information than linear data (e.g. Fabre et al. 2014; Cardini and Loy
128 2013), and thus this work expands and improves upon existing linear studies considering this clade
129 (Randau et al. 2016; Jones 2015). To our knowledge, two previous uses of 3D GMM to study the
130 shape of a complete vertebral region have been reported in the literature (e.g. the cervical region,
131 Werneburg 2015; Böhmer et al. 2015). While Böhmer et al. (2015) analysed individually landmarked
132 cervical vertebrae by plotting them together with a Principal Component Analyses, which described
133 main shape variation among those and allows for qualitative analyses of shape change across taxa,
134 Werneburg (2015) described a complex methodology that may not be broadly applicable.
135 Specifically, that method relied on finding landmarks on three-dimensional reconstructions which
136 had been matched to photographs of either manually articulated cervical vertebrae to approximate
137 *in vivo* orientations, or on model reconstructions of CT scans obtained from living animals. Those
138 conditions are not readily available for many taxa, and thus we believe that the approach described
139 here will be useful for a broader range of future studies. Additionally, Head and Polly (2015) used
140 two-dimensional landmarks to characterise the precoaclal axial skeleton of squamates; however, the
141 methodology described was applied to investigate patterns of regionalisation in the axial skeleton
142 instead of testing correlations between shape and ecology.

We first analyse the individual shape of selected vertebrae and test for the influence of factors known to affect the shape of skull and limbs, including size, locomotion and prey size specialisation (Carbone et al. 1999; Meachen-Samuels and Van Valkenburgh 2009a, 2009b). We then conduct separate analyses of each region of the vertebral column (cervical, thoracic, and lumbar regions, and hypothesized functional regions composed of different combinations of these regions), and assess shape differences and differential allometry associated with ecological groupings. Finally, we apply phenotypic trajectory analysis to the main dataset, a combined analysis of cervical, thoracic, and lumbar vertebrae, and also to individual regions with significant ecological signal, to analyse the shape of the vertebral column as a succession of contiguous units, thus overcoming the long-standing issue of analysing vertebrae as independent objects in geometric morphometric studies. We use these approaches to test the following hypotheses: 1) ecology is a significant influence on the morphology of felid vertebral column; and 2) vertebral regions display different levels of ecological and phylogenetic signal due to the regionalisation of shape in the mammalian vertebral column.

Material & Methods:

Data collection

In order to compose our 3D dataset, landmarks were collected from 19 presacral vertebrae from nine species of extant cats using an Immersion Microscribe G2X (Solution Technologies, Inc., Oella). This dataset included the following vertebrae: atlas, axis, C4, C6, C7, T1, T2, T4, T6, T8, T10, T11, T12, T13, L1, L2, L4, L6, and L7. As time constraints hindered the ability to collect dense data for every vertebra, but sufficient data were needed to describe the full presacral vertebral column morphology, the selection of these vertebrae was based on the following criteria: vertebrae with measurements that accounted for the highest principal component loadings in a previous linear study (Randau et al. 2016); vertebrae comprising the boundaries between vertebral regions and immediately preceding and succeeding vertebrae (e.g. C7 and T1, and C6 and T2, respectively); and

vertebrae which are thought to be of particular biomechanical importance (e.g. T11, the anticlinal vertebra). Landmarks were collected from 109 specimens, ranging from seven to 17 specimens per species, with the final dataset including a total of 1712 individual vertebrae (see Table S1 for specimen numbers). Analyses grouped these dataset in various ways, ranging from treating all vertebrae individually to pooling vertebrae in the most inclusive grouping (C4 – L7, excluding T11 – T13), as described further below. Vertebrae were also grouped into the following five regions for some analyses, including: C4 – T10, T1 – T10, T1 – L7, T10 – L7, and L1 – L7. These regions were selected because they correspond to or group clear anatomical regions (e.g., T1-T10, L1-L7, and T1-L7) or more inclusive regions demarked by anatomical transitions (i.e. anterior or posterior vertebral column defined by the dorsal limit of the diaphragm, e.g. C4 –T10 and T10 – L7, respectively; Gray et al. 2005; Buchholtz et al. 2012; Jones 2015).

Sixteen homologous landmarks were identified on 14 of these vertebrae (i.e. the post-atlanto-axial and pre-sacral C4 – L7 except for the T11-T13). 12 landmarks were gathered on C1 (atlas), and 14 on C2 (axis), due to their unique morphologies (Figure 1, and Table S2 of landmarks). Vertebrae T11 to T13 lack transverse processes and thus two out of the 16 selected landmarks (i.e. the right and left transverse process tips) could not be identified on those elements. Comparative analyses across all sampled vertebrae require all observations to have the same landmarks. For this reason, the majority of the following analyses, unless otherwise stated, only used the 14 vertebral types that contained the same 16 landmarks (Fig. 1D-I, i.e. not including the axis and atlas, shown on Fig. 1 A-B, and J-K respectively, due to their unique shape, or vertebrae T11 to T13).

In order to still include the T11-T13 vertebrae in our tests of ecological correlates of axial skeleton morphology, we conducted a second analysis using two alternative landmarks that represent the locations of the right and left accessory processes of these vertebrae (Fig. S1, landmarks 7 and 8). Accessory processes are slender processes that originate on the pedicle and extend posteriorly, laterally to each postzygapophyses, and reinforce the interzygapophyseal joint (De Iuliis and Pulerà

2007). Additionally, accessory processes were also present on vertebrae L1, L2 and L4 of all species analysed here. Therefore, the second analysis used the two accessory process landmarks instead of transverse process landmarks for the vertebrae T11 – L4, while the remaining vertebrae (C4- T10 and L6 - L7) continued to use the transverse processes landmarks. In this manner, a dataset of 16 landmarks was constructed for 17 vertebrae, although two of these landmarks are not homologous in all of the vertebrae.

As only the 14-vertebrae dataset (excluding C1-C2 and T11-T13) was composed of homologous landmarks, we focus on the 'multi-vertebrae' analyses of that dataset, hereafter referred to as the "homologous dataset" (or C4 – L7 for shortening, although not containing T11 – T13 as stated). The results from the alternative dataset that includes T11-T13 by using two non-homologous landmarks (accessory processes landmarks instead of transverse process landmarks for T11-L4), hereafter referred to as the "alternative dataset", were remarkably consistent and are presented in the supplementary information.

Ecological data for all analyses were collated from the literature (Meachen-Samuels and Van Valkenburgh 2009a, 2009b; Sunquist and Sunquist 2002). Prey size groupings include: small, mixed and large prey specialists. Locomotory groupings include: arboreal, cursorial, scansorial and terrestrial. Phylogenetic comparative analyses used the composite tree of Piras et al. (2013) pruned to the species sampled here.

Data analysis

All analyses were carried out in R version 3.2.2 (R Foundation 2015), using the 'geomorph' (Adams et al. 2015; Adams and Otarola-Castillo 2013), 'ape' (Paradis et al. 2004), and 'geiger' (Harmon et al. 2014) packages.

Prior to all subsequent analyses, missing landmarks due to broken specimens were imputed using the multivariate regression ("Reg") method in the 'estimate.missing' function of 'geomorph'. This

approach predicts the missing landmarks by using a multivariate regression of the specimen with missing values on all other landmarks in the set of complete specimens (Gunz et al. 2009). A total of 126 out of 30695 (0.41%) landmarks were imputed. All vertebrae were then subjected to Procrustes Superimposition within the relevant sample (i.e. either within same vertebral type sample, or specific vertebral region analysed depending on the analysis level) to remove any effects due to scale, rotation, and translation.

Phylogenetic and ecological signal of individual and regional vertebral shape

Preliminary analysis of vertebral column shape was performed with a combined Principal Component Analysis (PCA) of all of the vertebrae in the homologous landmark dataset (C4 – L7, excluding T11-T13). A second PCA was performed on the region encompassing vertebrae T10 – L7 in the homologous landmark dataset. Scans of individual cheetah (*Acinonyx jubatus*, USNM 520539) vertebrae were used to create an average reference mesh with the 'warpRefMesh' function in geomorph, and this mesh was used to warp the PC1 and PC2 minimum and maximum shapes in order to display vertebral shape changes across the main eigenvectors.

The effects of centroid size and ecological specialisation (both in terms of locomotion and prey size categories) on vertebral shape were evaluated with factorial MANOVAs of the vertebral Procrustes coordinates (i.e. shape ~ centroid size * ecology). Factorial MANOVAs with this size-ecology interaction accounts for the effect of 'size' while examining the other factors that describe shape and define the groups. Additionally, these non-parametric MANOVAs with 'RRPP' (residual randomization permutation procedure) allowed for significance tests with multidimensional data that have fewer observations than dimensions (Collyer et al. 2014). These analyses were performed separately on each vertebra from C1-L7, with each set composed of an across species pool (i.e., C1 dataset contained all C1 vertebrae measured, across all nine species) as well as on the complete homologous dataset (see supplementary information for further details on analyses of the alternative dataset). Additionally, factorial MANOVAs were applied to the five vertebral regions of described above, using

242 the homologous dataset. Each described region contained all vertebrae of the named types,
243 including all species listed here.

244 In order to assess the influence of phylogenetic relatedness on vertebral shape and centroid size (i.e.
245 whether more closely related species were more phenotypically similar; Felsenstein 1985), we first
246 constructed the mean shape for each individual vertebra (C1 to L7) per species and calculated the
247 phylogenetic signal with the 'Kmult' method (i.e. a multivariate version of the K-statistic; Adams
248 2014a) with the 'physignal' function in 'geomorph'. As L1-L4 have both transverse processes and
249 accessory processes and thus are the only elements with different landmarks in the homologous and
250 alternative datasets, this analysis was performed for both datasets for those elements. For individual
251 vertebrae that presented a significant phylogenetic signal in their shape across the studied species,
252 we also performed phylogenetic MANOVAs to assess the relationship between shape, centroid size
253 and ecological factors. Phylogenetic MANOVAs use a phylogeny-informed context under a Brownian
254 motion model of evolution to calculate a phylogenetic transformation matrix and the Gower-centred
255 distance matrix from predicted variable values, which are then used to asses significance from
256 comparisons between the values of statistical attributes obtained from those and the observed
257 values (Adams 2014b; Adams and Collyer 2015; Garland et al. 1993). Phylogenetic MANOVAs were
258 done using the 'procD.pgls' function in 'geomorph'.

259 *The interaction of allometry and ecology in vertebral regions*

260 Considering that previous studies of felid vertebral morphology have demonstrated the widespread
261 influence of allometry in vertebral linear dimensions (see below; Randau et al. 2016; Jones 2015;
262 Jones and Pierce 2015), we investigated whether prey size or locomotory ecomorphs presented
263 different allometries in their vertebral shape. Based on the MANOVA results (see below, and Table
264 5), the vertebral region with the highest absolute variance explained by the two ecological variables
265 (i.e. T10 – L7) was selected to examine differences in vertebral allometry with respect to ecological
266 specialisation.

Using the "PredLine" method of the 'plotAllometry' function in 'geomorph', the predicted allometric scores for these regions were calculated for each ecological group from the shape against centroid size regression. The method used produced allometric trajectories (i.e. plotted PC1 of the predicted values against size) which clearly exhibited allometric differences between ecological groups (Adams and Nistri 2010). The significance of the differences in the log centroid size ~ shape relationship between groups could be quantified by both the P value of the comparisons between slope distances, which itself measures differences in amount of shape change per unit of centroid size change, and the slope angle's P value, which indicates if the directions of these vectors point at different regions of the morphospace (Collyer et al. 2014; Collyer and Adams 2013). This last step was performed using the 'advanced.procD.lm' function in 'geomorph'.

Ecological signal across the vertebral column

Shape for the proxy of an entire vertebral column (i.e. C4 – L7, excluding T11 – T13), as well as for individual regions, was quantified using a novel application of Phenotypic Trajectory Analysis (PTA). PTA identifies a shape trajectory among associated data points (vertebrae, in this case) and then compares this trajectory among vertebra within each predetermined group (e.g. mean shape of C7 for all arboreal taxa), and then traces the trajectory between these means (e.g. C6 to C7, C7 to T1, etc.) (Adams and Collyer 2009, 2007; Collyer and Adams 2013). The trajectories can then be visualised in morphospace for a qualitative comparison between groupings, and differences in size, direction, and shape of the trajectories for each group can also be quantitatively compared. As above, taxa were grouped by prey size and locomotory categories for analysis of ecological signal in phenotypic trajectories.

Results:

Phylogenetic and ecological signal in individual and regional vertebral shape

The majority of the variance (90%) was summarised by the first four PCs in both the homologous and alternative datasets (Table 1, and Tables S3 and S4). PCA plots show three general morphological groupings: a C4 cluster, an 'end-cervicals' to T10 cluster (i.e. C6, C7, T1, T2, T4, T6, T8, and T10) and a lumbar cluster (i.e. L1, L2, L4, L6, and L7) (Fig. 2A-B and Fig. S2).

As noted in Methods, all of the following results refer to the homologous dataset unless otherwise indicated. The PC1 minimum shape was generally mediolaterally and anteroposteriorly compressed and dorsoventrally elongated, with smaller centrum width and centrum length, smaller distances between transverse processes, pre-zygapophyses, and post-zygapophyses, and larger heights for the centrum, neural canal, and neural spine. The PC1 maximum shape showed larger centrum width and centrum length, larger distances between transverse processes and intra-zygapophyses, but shorter heights for the centrum, neural canal, and neural spine. PC2, which separated the C4 cluster from the other two vertebral clusters, presented similar shape differences, with the PC2 minimum shape displaying even more exaggerated features related to mediolateral compression, but, in contrast, also exhibiting some anteroposterior elongation. The main feature of PC2's maximum shape was the relative augmentation of the distances in the mediolateral dimension, with larger centrum width and intra-zygapophyseal distances. Results from the PCA applied to the 'T10-L7' region (Table 2 and Table S5, see below) showed that the majority of the variation (>90%) was explained by the first five PCs, with PC1 explaining >60% of total variance.

When individual vertebral datasets were subjected to factorial MANOVAs of shape against centroid size, locomotion and prey size groups (Table 3), all vertebrae displayed significant correlations of shape with all three factors ($P < 0.001 – 0.05$), with the exception of the T8 x prey size ($P > 0.05$). After Bonferroni correction, only three correlations ceased from being significant (i.e. $P > 0.003$): C6 and T10 vs. prey size, and L7 vs. centroid size. The three examined factors explained a range between 3% and 23.77% of vertebral shape (highlighted on Table 3). Further, estimating the influence of evolutionary relatedness on vertebral shape recovered a significant (i.e. $P < 0.05$) phylogenetic signal

316 for the mean shape (i.e. Procrustes coordinates) of only five vertebrae: atlas, axis, C6, T1 and T2
317 (Table 4), however, after Bonferroni correction this signal was only significant for the atlas and axis
318 (i.e. $P < 0.003$). Conservatively, all of these five vertebrae were further subjected to a second round
319 of MANOVAs using the same factors as above, while controlling for this phylogenetic signal. After this
320 correction, none of ecological correlations were significant ($P >> 0.05$, Table 5).No phylogenetic
321 signal was recovered for centroid size of any of the analysed vertebrae.

322 Factorial MANOVAs were also applied to five regions composed of multiple vertebrae for
323 quantification of the influence of ecological factors on vertebral regions. The highest ecological signal
324 in vertebral shape was observed in the region from T10 to L7, with ~17.55% and ~12.2% of overall
325 shape explained by prey size and locomotory categories, respectively (see MANOVAs in Table 6 for all
326 results). This region also displayed the second highest values for the influence of centroid size on
327 shape (~7.8% Table 6). No significant correlation with locomotory categories was found for the
328 complete homologous dataset (C4 – L7) or for the C4-T10 region, while significant (i.e. both prior and
329 after Bonferroni correction) correlations with both locomotory and prey size groups were found for
330 the other regions but those ranged between 2.0 – 11.9% for locomotion and 1.6 – 12.6% for prey size
331 (Table 6).

332 *The interaction of allometry and ecology in vertebral regions*

333 As stated above, the interaction factor between ecological groups and centroid size was significant
334 and exhibited its highest values (Table 6) for the T10-L7 region, demonstrating that species belonging
335 to different ecological groups displayed distinct shape versus size relationships in the posterior
336 presacral vertebrae. Plots of the predicted allometric trajectories for each ecological factor on both
337 datasets are presented in Fig. 3A and B. The analysis using prey size groups for categorisation showed
338 that, while 'small' and 'big' prey size groups possessed allometric trajectories that were very similar
339 in slope distance ($P > 0.1$, Table 7), the 'mixed' prey size group's trajectory exhibited a slope distance
340 that was significantly different from both the large and small prey size groups ($P << 0.05$). However,

differences in the slope distance of the allometric trajectories between 'large' and 'mixed' prey size groups were not significant after Bonferroni correctior (i.e. $P > 0.006$). Slope angles were significantly different between the 'large' and 'small prey' categories, but not after Bonferroni correction. Grouping species by their locomotory modes resulted in allometric trajectories that were similar in slope distance between 'arboreal' and 'cursorial' groups ($P >> 0.05$), but both differed in all other pairwise comparisons between locomotory groups ($P << 0.05$). Slope angles were only significantly different between the 'terrestrial' and 'scansorial' subsets ($P << 0.05$).

Ecological signal across the vertebral column

Phenotypic trajectory analysis was first performed using the most inclusive homologous dataset (i.e. C4 – L7) to quantify the shape of the post-atlantoaxial presacral vertebral column (Table 8, and Fig. 4), followed by analysis of the T10 – L7 region. When species were grouped by prey size specialisation, phenotypic trajectories for the full dataset were significantly different in in shape. The 'small' prey size trajectory was also different from both the 'mixed' and 'big' prey size groups in terms of trajectory size. Grouping species by locomotory mode with the complete dataset was not performed because the MANOVA results for this region exhibited a non-significant correlation with locomotory groups ($P >> 0.05$, Table 6)).

Analysis of the T10-L7 vertebrae resulted in significant differences in phenotypic trajectories for both ecological factors (Table 9, and Fig. 5A and B). With prey size categorisation, the phenotypic trajectories were all significantly different in direction. The 'small' prey size trajectory was also different from both the 'mixed' and 'big' prey size groups in terms of shape. Locomotory group trajectories were different in direction for all pairwise comparisons, except between the 'scansorial' and 'terrestrial' groups. In terms of shape, the 'cursorial' phenotypic trajectory was statistically different from the 'arboreal' and 'scansorial' trajectories, but only before Bonferroni correction and not after ($P < 0.05$ but > 0.006, respectively).

Discussion:

When combined, analyses of the relationship among 3D vertebral shape, size, ecology, and phylogeny provide a more complete understanding of the forces shaping the evolution of the felid vertebral column evolution. The results reported here have confirmed our initial hypotheses on ecological drivers in the vertebral column shape differentiation in felids, and we have detailed how specialisation towards the observed ecologies correlates with regionalisation of the presacral axial skeleton. While vertebrae in the anterior-most region of the felids' vertebral columns (i.e. atlas and axis, but also C6, T1, and T2) were more phylogenetically conservative in shape, the posterior regions of the vertebral column showed a stronger influence of ecological specialisations. That the strongest size and ecology correlations are observed in this more caudal region of the presacral vertebral column (i.e. T10 – L7; see Supplementary information for similar results on the dataset using the accessory processes landmarks) supports the inference that this region may be subjected to stronger selection, or equally to weaker evolutionary constraints, and might present greater evolutionary respondability across felids, or even more broadly. This observation agrees with the work by Jones and German (2014), in which they found that, in mammals, centrum length varied the most in the lumbar region both through ontogeny and interspecifically. As an osteological measurement that is informative towards the degree of passive robustness at intervertebral joints (Pierce et al. 2011; Shapiro 1995; Shapiro 2007; Koob and Long 2000), centrum length can be used to make inferential comparisons of resistance to intervertebral bending and general biomechanical properties between species or ecological groups. An additional PCA limited to the T10-L7 vertebrae (post-diaphragmatic homologous dataset) (Fig. 2C) shows that the anteroposterior vertebral axis, which primarily represents centrum length, is one of the main contributors to variation in this dataset.

When compared to our previous work on the linear morphological change in the felid axial skeleton (Randau et al. 2016), our present study supports our general conclusions of regionalisation of ecological signal in the vertebral column, with stronger locomotory signal present in the posterior region. However, contrary to results from linear data (Randau et al. 2016), the 3D analyses described here also found a significant correlation between vertebral morphology and prey size specialisation.

Previous studies of individual vertebral attributes (e.g. centrum length) and different proxies for body size (e.g. total vertebral length, body mass) using length measurements have also identified significant allometry across felids (Randau et al. 2016; Jones 2015). Here, we were interested in investigating whether the influence of size (i.e. centroid size) on vertebral multidimensional shape was also regionalised, and most importantly, whether such scaling relationships differed with ecology. Our results reinforce the conclusion that size influences vertebral shape throughout the axial skeleton (i.e. C4 and post-T2 vertebrae), but that these size effects are strongest in T10 and the lumbars (Tables 3 and 6, and in the last thoracics in Table S6). Additionally, we have demonstrated that ecological specialists, especially in terms of locomotory specialisation, indeed exhibit a distinct scaling relationship between shape and centroid size (Table 7). Observed differences between prey size subsets were very consistent with both measures of differentiation (slope angle and distance). 'Small' and 'mixed' prey size groups were shown to have distinct allometric vertebral shapes. Although 'large' and 'small' prey groups were not significantly different in terms of the intensity of their allometries (i.e. the Procrustes distances between slopes), they displayed distinct angles in their slope vector, showing that the covariances between the variables are different in these ecological categories (Collyer and Adams 2013; Adams and Collyer 2009). However, these differences between 'large' and 'small' categories, or regarding the intensity of the allometry between 'large' and 'mixed' categories, were not significant after correction, suggesting differences in allometry between prey size specialist groups might be subtle. This could therefore be one of the factors which caused linear measurements were not to be successful in finding correlations between felid vertebral morphology and specialisation towards prey size (Randau et al. 2016). With regards to locomotory specialisation, the two statistical attributes presented different patterns. A better separation between the groups was found in terms of the intensity of their allometries than in their directions. Additionally, it is clear from the observation of regression slopes (Fig. 3B) that allometric shape changes are much greater in 'arboreal' and 'cursorial' species and, although significant, size-related changes in the posterior vertebral morphology are less demarked in 'scansorial' and 'terrestrial' felids. Although all but one

418 pairwise comparisons were significantly different with regards to slope distance, the only significant
419 difference in the direction of the allometric trajectories was found between the 'terrestrial' and
420 'scansorial' categories. Hence, although these two more generalist locomotory groups show a
421 comparatively smaller degree of vertebral allometric scaling, they are still distinct in the relative way
422 size influence vertebral shape variables.

423 As nearly all individual vertebrae showed some significant correlation between shape and ecology
424 (i.e. Table 3), individual analyses alone provide little clarity in terms of regionalisation of ecological
425 and phylogenetic signals. Such differentiation was only possible when sets of vertebrae were
426 analysed together through PTA. With this method, we were able to quantitatively differentiate the
427 vertebral shape gradient changes between locomotor and prey size specialist felid species, therefore
428 extracting the subtle morphological changes between the recognised ecomorphs in this
429 phenotypically-conserved clade.

430 Of the two ecological factors examined in this study, only prey size specialisation as an isolated factor
431 exhibited a significant correlation with total vertebral column shape, contrary to the results of linear
432 analyses (Randau et al. 2016). This result once again supports the regionalisation of locomotory
433 specialisation in the vertebral column, which was instead found to significantly correlate only to
434 more posterior regions, while also highlighting the increased resolution provided by 3D data.
435 However, because prey size specialisation is directly correlated to the species' body mass (Carbone et
436 al. 1999; Carbone et al. 2007), a significant correlation between this factor and vertebral shape is
437 possibly an indirect reflection of overall body size influence on vertebral 3-dimensional shape.

438 When we focused our analyses on the vertebral regions with highest correlations between shape and
439 the factors examined, the T10 – L7 trajectories were best able to separate among ecological groups,
440 both for the locomotion and prey size categories (Fig. 5A-B). All significant differences between
441 trajectories were found in comparisons of the shape and direction of those trajectories (Table 9). This
442 result suggests that no differences in the amount of shape variation (i.e. trajectory size) were found

443 in the species of felids studied here. Additionally, this differentiation in trajectory direction implies
444 that the differences found were primarily based on the distinct relative covariations of vertebral
445 shape variables between ecological groups throughout the vertebral column (Collyer and Adams
446 2013; Adams and Collyer 2009). More interestingly put, these differences in trajectory direction
447 between groups are evidence of ecological divergence between those groups (Adams et al. 2013;
448 Stayton 2006). As it follows, the only two groups that did not differ significantly in trajectory
449 direction (the 'scansorial' and 'terrestrial' groups) show ecological convergence in the shape of the
450 posterior vertebral column.

451 Combining the PTA and posterior region PCA results (Fig. 2C) provides additional information on the
452 changes in vertebral morphology correlated with cursoriality in felids. Cheetahs (*Acinonyx jubatus*),
453 as the species represented by the 'cursorial' locomotory group, presented an average lumbar
454 morphology that exhibited longer centra, and overall less shortening of the centrum from L1 to L7,
455 which could be visualised by the trajectory lumbar points presenting lower values on PC1, and higher
456 values on PC2 (Fig. 5B). The relative length of centra has been shown to be associated with the
457 degree of flexibility between two consecutive vertebrae (Koob & Long, 2000; Long et al., 1997;
458 Pierce, Clack & Hutchinson, 2011), and results from a study by Jones (2015) on linear vertebral
459 dimensions revealed allometric shortening of the lumbar region in felids (but see Randau et al. 2016
460 for alternative results showing isometric scaling of the lumbar region in this family, albeit with a
461 different sample). Ergo, having lumbar vertebrae that are relatively longer might indeed contribute
462 to greater sagittal bending, and contribute to having the longer stride lengths observed in this highly
463 specialised felid (Hildebrand 1959).

464

465 **Conclusion**

466 The vertebral column has been underrepresented in the functional morphology and morphometric
467 literature, but recent studies have shown that vertebral form carries rich developmental and

ecomorphological signals. Here, through multivariate statistical analyses, we have demonstrated that the use of geometric morphometrics to study the axial skeleton can offer even more detailed ecomorphological information than what has been reported by linear studies. Additionally, we have here provided the first application of a method that allows for the shape analysis of a contiguous sequence of vertebrae as functionally linked osteological structures.

We have shown that ecological correlates influence the shape of the vertebral column heterogeneously, specifically with discrete regions such as the posterior axial skeleton presenting higher correlation with both locomotory and prey size specialisation. Furthermore, we suggest that the post-T10 vertebrae may be the most ecologically adaptable region among felid species. While anterior vertebrae may either have evolved under stronger phylogenetic constraints or are more ecologically conservative, posterior vertebrate show clearer differentiation between ecomorphs in Felidae.

Future studies, which may benefit from focusing on a more restricted species range, or on smaller vertebral regions, would gain from including vertebrae that were not analysed here in order to compare the general patterns found to specific complete regional trends.

Conflict of Interests

The authors declare no conflict of interest.

References:

Adams, D. C. (2014a). A generalized K statistic for estimating phylogenetic signal from shape and other high-dimensional multivariate data. *Systematic Biology, 63*(5), 685-697, doi:10.1093/sysbio/syu030.

Adams, D. C. (2014b). A method for assessing phylogenetic least squares models for shape and other high-dimensional multivariate data. *Evolution, 68*(9), 2675-2688, doi:10.1111/evo.12463.

493 Adams, D. C., & Collyer, M. L. (2007). Analysis of character divergence along environmental gradients
494 and other covariates. *Evolution, 61*(3), 510-515, doi:10.1111/j.1558-5646.2007.00063.x.
495 Adams, D. C., & Collyer, M. L. (2009). A general framework for the analysis of phenotypic trajectories
496 in evolutionary studies. *Evolution, 63*(5), 1143-1154, doi:10.1111/j.1558-5646.2009.00649.x.
497 Adams, D. C., & Collyer, M. L. (2015). Permutation tests for phylogenetic comparative analyses of
498 high-dimensional shape data: what you shuffle matters. *Evolution and Development, 69*(3),
499 823-829, doi:10.1111/evo.12596.
500 Adams, D. C., & Nistri, A. (2010). Ontogenetic convergence and evolution of foot morphology in
501 European cave salamanders (Family: Plethodontidae). *BMC Evol Biol, 10*, 216,
502 doi:10.1186/1471-2148-10-216.
503 Adams, D. C., & Otarola-Castillo, E. (2013). geomorph: an R package for the collection and analysis of
504 geometric morphometric shape data. *Methods Ecol Evol, 4*, 393-399.
505 Adams, D. C., Rohlf, F. J., & Slice, D. E. (2013). A field comes of age: geometric morphometrics in the
506 21st century. *Hystrix, 24*(1), 1:10, doi:10.4404/hystrix-24.1-6283.
507 Adams, D. S., Collyer, M., & Sherrat, E. (2015). geomorph: Software for geometric morphometric
508 analyses. R package version 2.1.x. (2.1.x ed.).
509 Alvarez, A., Ercoli, M. D., & Prevosti, F. J. (2013). Locomotion in some small to medium-sized
510 mammals: a geometric morphometric analysis of the penultimate lumbar vertebra, pelvis
511 and hindlimbs. *Zoology (Jena), 116*(6), 356-371, doi:10.1016/j.zool.2013.08.007.
512 Andersson, K., & Werdelin, L. (2003). The evolution of cursorial carnivores in the Tertiary:
513 implications of elbow-joint morphology. *Proceedings of Royal Society of London B, 270 Suppl*
514 *2*, S163-165, doi:10.1098/rsbl.2003.0070.
515 Arnold, P., Forterre, F., Lang, J., & Fischer, M. S. (2016). Morphological disparity, conservatism, and
516 integration in the canine lower cervical spine: Insights into mammalian neck function and
517 regionalization. *Mammalian Biology, 81*(2), 153-162, doi:10.1016/j.mambio.2015.09.004.
518 Bell, E., Andres, B., & Goswami, A. (2011). Integration and dissociation of limb elements in flying
519 vertebrates: a comparison of pterosaurs, birds and bats. *J Evol Biol, 24*(12), 2586-2599,
520 doi:10.1111/j.1420-9101.2011.02381.x.
521 Bennett, V. C., & Goswami, A. (2011). Does developmental strategy drive limb integration in
522 marsupials and monotremes? *Mammalian Biology, 76*(1), 79-83,
523 doi:10.1016/j.mambio.2010.01.004.
524 Benoit, M. H. (2010). What's the difference? A multiphasic allometric analysis of fossil and living
525 lions. In A. Goswami, & A. Friscia (Eds.), *Carnivoran evolution: New views on phylogeny, form*
526 *and function* (pp. 165-188). Cambridge: Cambridge University Press.
527 Böhmer, C., Rauhut, O. W., & Wörheide, G. (2015). Correlation between Hox code and vertebral
528 morphology in archosaurs. *Proceedings of the Royal Society B, 282*(1810),
529 doi:10.1098/rspb.2015.0077.
530 Boszczyk, B. M., Boszczyk, A. A., & Putz, R. (2001). Comparative and functional anatomy of the
531 mammalian lumbar spine. *Anatomical Records, 264*, 157–168.
532 Breit, S., & Künzel, W. (2004). A morphometric investigation on breed-specific features affecting
533 sagittal rotational and lateral bending mobility in the canine cervical spine (C3-C7).
534 *Anatomia, Histologia, Embryologia, 33*(4), 244-250.
535 Buchholtz, E. A. (2001a). Swimming styles in Jurassic ichthyosaurs. *Journal of Vertebrate*
536 *Paleontology, 21*, 61-73.
537 Buchholtz, E. A. (2001b). Vertebral osteology and swimming style in living and fossil whales (Order:
538 Cetacea). *Journal of Zoology, 253*, 175-190.
539 Buchholtz, E. A. (2014). Crossing the frontier: a hypothesis for the origins of meristic constraint in
540 mammalian axial patterning. *Zoology (Jena), 117*(1), 64-69, doi:10.1016/j.zool.2013.09.001.
541 Buchholtz, E. A., Bailin, H. G., Laves, S. A., Yang, J. T., Chan, M. Y., & Drozd, L. E. (2012). Fixed cervical
542 count and the origin of the mammalian diaphragm. *Evolution and Development, 14*(5), 399-
543 411, doi:10.1111/j.1525-142X.2012.00560.x.

544 Buchholtz, E. A., Wayrynen, K. L., & Lin, I. W. (2014). Breaking constraint: axial patterning in
545 *Trichechus* (Mammalia: Sirenia). *Evolution and Development, 16*(6), 382-393.
546 Carbone, C., Mace, G. M., Roberts, S. C., & Macdonald, D. W. (1999). Energetic constaints on the diet
547 of terrestrial carnivores. *Nature, 402*, 286-288.
548 Carbone, C., Teacher, A., & Rowcliffe, J. M. (2007). The costs of carnivory. *PLoS Biol, 5*(2), e22,
549 doi:10.1371/journal.pbio.0050022.
550 Cardini, A., & Loy, A. (2013). On growth and form in the "computer area": from geometric to
551 biological morphometrics. *Hystrix, 24*(1), 1-5, doi:10.4404/hystrix-24.1-8749.
552 Chatzigianni, A., & Halazonetis, D. J. (2009). Geometric morphometric evaluation of cervical
553 vertebrae shape and its relationship to skeletal maturation. *American Journal of Orthodontics*
554 *and Dentofacial Orthopedics, 136*(4), 481.e481-481.e489.
555 Chen, X., Milne, N., & O'Higgins, P. (2005). Morphological variation of the thoracolumbar vertebrae in
556 Macropodidae and its functional relevance. *J Morphol, 266*(2), 167-181.
557 Collyer, M. L., & Adams, D. C. (2013). Phenotypic trajectory analysis: comparison of shape change
558 patterns in evolution and ecology. *Hystrix, 24*(1), 75–83, doi:10.4404/hystrix-24.1-6298.
559 Collyer, M. L., Sekora, D. J., & Adams, D. C. (2014). A method for analysis of phenotypic change for
560 phenotypes described by high-dimensional data. *Heredity*, doi:10.1038/hdy.2014.75.
561 Cuff, A. R., Sparkes, E. L., Randau, M., Pierce, S. E., Kitchener, A. C., Goswami, A., et al. (2016a). The
562 scaling of postcranial muscles in cats (Felidae) I: forelimb, cervical, and thoracic muscles. *J*
563 *Anat, 229*(1), 128-141, doi:10.1111/joa.12477.
564 Cuff, A. R., Sparkes, E. L., Randau, M., Pierce, S. E., Kitchener, A. C., Goswami, A., et al. (2016b). The
565 scaling of postcranial muscles in cats (Felidae) II: hindlimb and lumbosacral muscles. *J Anat,*
566 *229*(1), 142-152, doi:10.1111/joa.12474.
567 Davies, T. J., Meiri, S., Barraclough, T. G., & Gittleman, J. L. (2007). Species co-existence and character
568 divergence across carnivores. *Ecol Lett, 10*(2), 146-152, doi:10.1111/j.1461-
569 0248.2006.01005.x.
570 Day, L. M., & Jayne, B. C. (2007). Interspecific scaling of the morphology and posture of the limbs
571 during the locomotion of cats (Felidae). *Journal of Experimental Biology, 210*(4), 642-654,
572 doi:10.1242/jeb.02703.
573 De Iuliis, G., & Pulerà, D. (2007). The cat. In *The dissection of vertebrates: a laboratory manual* (pp.
574 131-226): Academic Press.
575 Doube, M., Wiktorowicz-Conroy, A., Christiansen, P., Hutchinson, J. R., & Shefelbine, S. (2009). Three-
576 dimensional geometric analysis of felid limb bone allometry. *PLoS One, 4*(3), e4742,
577 doi:10.1371/journal.pone.0004742.
578 Drake, A. G., & Klingenberg, C. P. (2010). Large-scale diversification of skull shape in domestic dogs:
579 disparity and modularity. *Am Nat, 175*(3), 289-301, doi:10.1086/650372.
580 Dumont, M., Wall, C. E., Botton-Divet, L., Goswami, A., Peigne, S., & Fabre, A. C. (2015). Do functional
581 demands associated with locomotor habitat, diet, and activity pattern drive skull shape
582 evolution in musteloid carnivorans? *Biological Journal of the Linnean Society, 117*(4), 858-
583 878, doi:10.1111/bij.12719.
584 Ercoli, M. D., Prevosti, F. J., & ÁLvarez, A. (2012). Form and function within a phylogenetic
585 framework: locomotory habits of extant predators and some Miocene Sparassodonta
586 (Metatheria). *Zoological Journal of the Linnean Society, 165*(1), 224-251, doi:10.1111/j.1096-
587 3642.2011.00793.x.
588 Fabre, A. C., Cornette, R., Huyghe, K., Andrade, D. V., & Herrel, A. (2014). Linear versus geometric
589 morphometric approaches for the analysis of head shape dimorphism in lizards. *J Morphol,*
590 *275*(9), 1016-1026, doi:10.1002/jmor.20278.
591 Fabre, A. C., Cornette, R., Peigne, S., & Goswami, A. (2013). Influence of body mass on the shape of
592 forelimb in musteloid carnivorans. *Biological Journal of the Linnean Society, 110*(1), 91-103,
593 doi:Doi 10.1111/Bij.12103.
594 Felsenstein, J. (1985). Phylogenies and the comparative method. *Am Nat, 125*(1), 1-15.

595 Figueirido, B., Serrano-Alarcon, F. J., Slater, G. J., & Palmqvist, P. (2010). Shape at the cross-roads:
596 homoplasy and history in the evolution of the carnivoran skull towards herbivory. *J Evol Biol,*
597 *23*(12), 2579-2594, doi:10.1111/j.1420-9101.2010.02117.x.
598 Finch, M., & Freedman, L. (1986). Functional-morphology of the vertebral column of *Thylacoleo*
599 *carnifex* Owen (Thylacoleonidae, Marsupialia). *Aust J Zool, 34*, 1-16.
600 Foth, C., Brusatte, S. L., & Butler, R. J. (2012). Do different disparity proxies converge on a common
601 signal? Insights from the cranial morphometrics and evolutionary history of Pterosauria
602 (Diapsida: Archosauria). *J Evol Biol, 25*(5), 904-915, doi:10.1111/j.1420-9101.2012.02479.x.
603 Gál, J. M. (1993). Mammalian spinal biomechanics II. Intervertebral lesion experiments and
604 mechanisms of bending resistance. *Journal of Experimental Biology, 174*, 281-297.
605 Galis, F., Carrier, D. R., van Alphen, J., van der Mije, S. D., Van Dooren, T. J., Metz, J. A., et al. (2014).
606 Fast running restricts evolutionary change of the vertebral column in mammals. *Proceedings*
607 *of the National Academy of Science USA, 111*(31), 11401-11406,
608 doi:10.1073/pnas.1401392111.
609 Garland, T., Jr., Dickerman, A. W., Janis, C. M., & Jones, J. A. (1993). Phylogenetic Analysis of
610 Covariance by Computer Simulation. *Systematic Biology, 42*(3), 265-292.
611 Gonyea, W. J. (1978). Functional implications of felid forelimb anatomy. *Acta Anatomica (Basel),*
612 *102*(2), 111-121.
613 Goswami, A. (2006). Morphological integration in the carnivoran skull. *Evolution, 60*(1), 15.
614 Goswami, A., & Polly, P. D. (2010). The influence of character correlations of phylogenetic analyses: a
615 case study of the carnivoran cranium. In A. Goswami, & A. Friscia (Eds.), *Carnivoran*
616 *evolution: New views on phylogeny, form, and function.* (pp. 141-164). Cambridge:
617 Cambridge University Press.
618 Goswami, A., Polly, P. D., Mock, O. B., & Sanchez-Villagra, M. R. (2012). Shape, variance and
619 integration during craniogenesis: contrasting marsupial and placental mammals. *J Evol Biol,*
620 *25*(5), 862-872, doi:10.1111/j.1420-9101.2012.02477.x.
621 Goswami, A., Smaers, J. B., Soligo, C., & Polly, P. D. (2014). The macroevolutionary consequences of
622 phenotypic integration: from development to deep time. *Philosophical transactions of the*
623 *Royal Society B, 369*(1649), 1-15, doi:10.1098/rstb.2013.0254.
624 Gould, S. J. (1966). Allometry and size in ontogeny and phylogeny. *Biological Reviews, 41*, 52.
625 Gray, H., Standring, S., Ellis, H., & Berkovitz, B. (2005). *Gray's Anatomy: The Anatomical Basis of*
626 *Clinical Practice.* (39th ed.). Edinburgh: Churchill Livingstone: Elsevier.
627 Gunz, P., Mitteræcker, P., Neubauer, S., Weber, G. W., & Bookstein, F. L. (2009). Principles for the
628 virtual reconstruction of hominin crania. *Journal of Human Evolution, 57*, 48-62.
629 Harmon, L., Weir, J., Brock, C., Glor, R., Challenger, W., Hunt, G., et al. (2014). Analysis of
630 evolutionary diversification. (2.0.6 ed., pp. Methods for fitting macroevolutionary models to
631 phylogenetic trees.).
632 Head, J. J., & Polly, P. D. (2015). Evolution of the snake body form reveals homoplasy in amniote Hox
633 gene function. *Nature, 520*(7545), 86-89, doi:10.1038/nature14042.
634 Hildebrand, M. (1959). Motions of the running cheetah and horse. *Journal of Mammalogy, 40*(4),
635 481-495.
636 Hua, S. (2003). Locomotion in marine mesosuchians (Crocodylia): the contribution of the 'locomotion
637 profiles'. *Neues jahrbuch für geologie und palaontologie abhandlungen, 227*, 139-152.
638 Johnson, D. R., McAndrew, T. J., & Oguz, O. (1999). Shape differences in the cervical and upper
639 thoracic vertebrae in rats (*Rattus norvegicus*) and bats (*Pteropus poiocephalus*): can we see
640 shape patterns derived from position in column and species membership ? *J Anat, 194*(2),
641 249-253.
642 Jones, K. E. (2015). Evolutionary allometry of the thoracolumbar centra in felids and bovids. *J*
643 *Morphol, 276*(7), 818-831, doi:10.1002/jmor.20382.

644 Jones, K. E., & German, R. Z. (2014). Ontogenetic allometry in the thoracolumbar spine of mammal
645 species with differing gait use. *Evolution and Development, 16*(2), 110-120,
646 doi:10.1111/ede.12069.
647 Jones, K. E., & Pierce, S. E. (2015). Axial allometry in a neutrally buoyant environment: Effects of the
648 terrestrial-aquatic transition on vertebral scaling. *J Evol Biol, 29*(3), 594-601,
649 doi:10.1111/jeb.12809.
650 Klingenberg, C. P., & Marugán-Lobón, J. (2013). Evolutionary Covariation in Geometric Morphometric
651 Data: Analyzing Integration, Modularity, and Allometry in a Phylogenetic Context. *Systematic*
652 *Biology, 62*(4), 591–610, doi:10.1093/sysbio/syt025.
653 Koob, T. J., & Long, J. H. (2000). The vertebrate body axis: Evolution and mechanical function.
654 *American Zoologist, 40*(1), 1-18, doi:Doi 10.1668/0003-1569(2000)040[0001:Tvbaea]2.0.Co;2.
655 Lauder, G. V. (1995). On the inference of function from structure. In J. J. Thomason (Ed.), *Functional*
656 *anatomy of vertebrates: an evolutionary perspective.* (pp. 11 - 18). Cambridge: Cambridge
657 University Press.
658 Long, J. H., Jr., Pabst, D. A., Shepherd, W. R., & McLellan, W. A. (1997). Locomotor design of dolphin
659 vertebral columns: bending mechanics and morphology of Delphinus delphis. *Journal of*
660 *Experimental Biology, 200*, 65-81.
661 Macpherson, J. M., & Fung, J. (1998). Activity of thoracic and lumbar epaxial extensors during
662 postural responses in the cat. *Experimental Brain Research, 119*(3), 315-323, doi:DOI
663 10.1007/s002210050347.
664 Manfreda, E., Mitterœcker, P., Bookstein, F. L., & Schæfer, K. (2006). Functional morphology of the
665 first cervical vertebra in humans and nonhuman primates. *The Anatomical Record, 289B*(5),
666 184-194.
667 Martin-Serra, A., Figueirido, B., & Palmqvist, P. (2014). A three-dimensional analysis of morphological
668 evolution and locomotor performance of the carnivoran forelimb. *PLoS One, 9*(1), e85574,
669 doi:10.1371/journal.pone.0085574.
670 Meachen-Samuels, J., & Van Valkenburgh, B. (2009a). Craniodental indicators of prey size preference
671 in the Felidae. *Biological Journal of the Linnean Society, 96*(4), 784-799, doi:DOI
672 10.1111/j.1095-8312.2008.01169.x.
673 Meachen-Samuels, J., & Van Valkenburgh, B. (2009b). Forelimb indicators of prey-size preference in
674 the Felidae. *J Morphol, 270*(6), 729-744, doi:10.1002/jmor.10712.
675 Meachen, J. A., O'Keefe, F. R., & Sadleir, R. W. (2014). Evolution in the sabre-tooth cat,*Smilodon*
676 *fatalis*, in response to Pleistocene climate change. *J Evol Biol, 27*(4), 714-723,
677 doi:10.1111/jeb.12340.
678 Mitteroecker, P., & Gunz, P. (2009). Advances in Geometric Morphometrics. *Evolutionary Biology,*
679 *36*(2), 235-247, doi:10.1007/s11692-009-9055-x.
680 Mitteroecker, P., Gunz, P., Windhager, S., & Schæfer, K. (2013). A brief review of shape, form, and
681 allometry in geometric morphometrics, with applications to human facial morphology.
682 *Hystrix, 21*(1), 59-66, doi:10.4404/hystrix-24.1-6369.
683 Molnar, J. L., Pierce, S. E., Bhullar, B.-A. S., Turner, A. H., & Hutchinson, J. R. (2015). Morphological
684 and functional changes in the vertebal column with increasing aquactic adaptation in
685 crocodylomorphs. *Royal Society Open Science, 2*, 1-22, doi:10.1098/rsos.150439.
686 Monteiro, L. R. (2013). Morphometrics and the comparative method: studying the evolution of
687 biological shape. *Hystrix, 24*(1), 25-32, doi:10.4404/hystrix-24.1-6282.
688 Müller, J., Scheyer, T. M., Head, J. J., Barrett, P. M., Werneburg, I., Ericson, P. G., et al. (2010).
689 Homeotic effects, somitogenesis and the evolution of vertebral numbers in recent and fossil
690 amniotes. *Proceedings of the National Academy of Science USA, 107*(5), 2118–2123,
691 doi:10.1073/pnas.0912622107.
692 Narita, Y., & Kuratani, S. (2005). Evolution of the vertebral formulae in mammals: a perspective on
693 developmental constraints. *Journal of Experimental Zoology Part B: Molecular and*
694 *Developmental Evolution, 304*(2), 91-106, doi:10.1002/jez.b.21029.

Paradis, E., Claude, J., & Strimmer, K. (2004). APE: analyses of phylogenetics and evolution in R language. *Bioinformatics, 20*, 289-290, doi:doi:10.1093/bioinformatics/btg412.
Pierce, S. E., Angielczyk, K. D., & Rayfield, E. J. (2008). Patterns of morphospace occupation and mechanical performance in extant crocodilian skulls: a combined geometric morphometric and finite element modeling approach. *J Morphol, 269*(7), 840-864, doi:10.1002/jmor.10627.
Pierce, S. E., Angielczyk, K. D., & Rayfield, E. J. (2009). Shape and mechanics in thalattosuchian (Crocodylomorpha) skulls: implications for feeding behaviour and niche partitioning. *J Anat, 215*(5), 555-576, doi:10.1111/j.1469-7580.2009.01137.x.
Pierce, S. E., Clack, J. A., & Hutchinson, J. R. (2011). Comparative axial morphology in pinnipeds and its correlation with aquatic locomotory behaviour. *J Anat, 219*(4), 502-514, doi:10.1111/j.1469-7580.2011.01406.x.
Piras, P., Maiorino, L., Teresi, L., Meloro, C., Lucci, F., Kotsakis, T., et al. (2013). Bite of the cats: Relationships between functional integration and mechanical performance as revealed by mandible geometry. *Systematic Biology, 62*(6), 878–900, doi:10.1093/sysbio/syt053.
Polly, P. D., Lawing, A. M., Fabre, A. C., & Goswami, A. (2013). Phylogenetic principal components analysis and geometric morphometrics. *Hystrix, 24*(1), 33-41, doi:10.4404/hystrix-24.1-6383.
R Foundation (2015). The R Project for Statistical Computing. (3.2.3 ed.).
Randau, M., Goswami, A., Hutchinson, J. R., Cuff, A. R., & Pierce, S. E. (2016). Cryptic complexity in felid vertebral evolution: shape differentiation and allometry of the axial skeleton. *Zoological Journal of the Linnean Society, 178*(1), 183-202, doi:10.1111/zoj.12403.
Rudwick, M. J. S. (2005). Denizens of a former world. In M. J. S. Rudwick (Ed.), *Bursting the limits of time: The reconstruction of geohistory in the age of revolution* (pp. 349-416). Chicago: The University of Chicago Press.
Schilling, N., & Long, J. H., Jr. (2014). Axial systems and their actuation: new twists on the ancient body of craniates. *Zoology (Jena), 117*(1), 1-6, doi:10.1016/j.zool.2013.11.002.
Sears, K. E., Bianchi, C., Powers, L., & Beck, A. L. (2013). Integration of the mammalian shoulder girdle within populations and over evolutionary time. *J Evol Biol, 26*(7), 1536-1548, doi:10.1111/jeb.12160.
Shapiro, L. (1995). Functional morphology of indrid lumbar vertebrae. *Am J Phys Anthropol, 98*(3), 323-342, doi:10.1002/ajpa.1330980306.
Shapiro, L. J. (2007). Morphological and functional differentiation in the lumbar spine of lorisids and galagids. *Am J Primatol, 69*(1), 86-102, doi:10.1002/ajp.20329.
Sheets, H. D., & Zelditch, M. L. (2013). Studying ontogenetic trajectories using resampling methods and landmark data. *Hystrix, 24*(1), 67 -73, doi:10.4404/hystrix-24.1-6332.
Slater, G. J., & Van Valkenburgh, B. (2008). Long in the tooth: evolution of sabertooth cat cranial shape. *Paleobiology, 34*(3), 403-419, doi:Doi 10.1666/07061.1.
Smeathers, J. E. (1981). *A mechanical analysis of the mammalian lumbar spine.* Thesis dissertation., University of Reading,
Stayton, C. T. (2005). Morphological evolution of the lizard skull: a geometric morphometrics survey. *J Morphol, 263*(1), 47-59, doi:10.1002/jmor.10288.
Stayton, C. T. (2006). Testing hypotheses of convergence with multivariate data: morphological and functional convergence among herbivorous lizards. *Evolution, 60*(4), 824-841, doi:10.1554/04-575.1.s1.
Sunquist, M., & Sunquist, F. (2002). *Wild Cats of the World*: University of Chicago Press.
Walmsley, A., Elton, S., Louys, J., Bishop, L. C., & Meloro, C. (2012). Humeral epiphyseal shape in the felidae: the influence of phylogeny, allometry, and locomotion. *J Morphol, 273*(12), 1424-1438, doi:10.1002/jmor.20084.
Ward, A. B., & Mehta, R. S. (2014). Differential occupation of axial morphospace. *Zoology (Jena), 117*(1), 70-76, doi:10.1016/j.zool.2013.10.006.
Wellik, D. M. (2007). Hox patterning of the vertebrate axial skeleton. *Developmental Dynamics, 236*(9), 2454-2463, doi:10.1002/dvdy.21286.

746 Werneburg, I. (2015). Neck motion in turtles and its relation to the shape of the temporal skull
747 region. *Comptes Rendus de l'Académie des Sciences Series IIA Earth and Planetary Science,*
748 *14*(6-7), 527-548, doi:10.1016/j.crpv.2015.01.007.
749 Werneburg, I., Wilson, L. A., Parr, W. C., & Joyce, W. G. (2015). Evolution of neck vertebral shape and
750 neck retraction at the transition to modern turtles: an integrated geometric morphometric
751 approach. *Systematic Biology, 64*(2), 187-204, doi:10.1093/sysbio/syu072.
752 Zhang, K. Y., Wiktorowicz-Conroy, A., Hutchinson, J. R., Doube, M., Klosowski, M., Shefelbine, S. J., et
753 al. (2012). 3D Morphometric and posture study of felid scapulae using statistical shape
754 modelling. *PLoS One, 7*(4), 771-784, doi:10.1371/journal.pone.0034619.

755

756

757

Figure legends:

Figure 1: Different vertebral morphologies and their respective three-dimensional landmarks: (A-C) atlas in anterior, posterior and dorsal view; (D-F) T1 in anterior, posterior and lateral view; (G-I) L1 in anterior, posterior and lateral view; and (J-K) axis in anterior and posterior view. Vertebral images are from CT scans of *Acinonyx jubatus* (Cheetah, USNM 520539). Landmark descriptions can be found in Table S2.

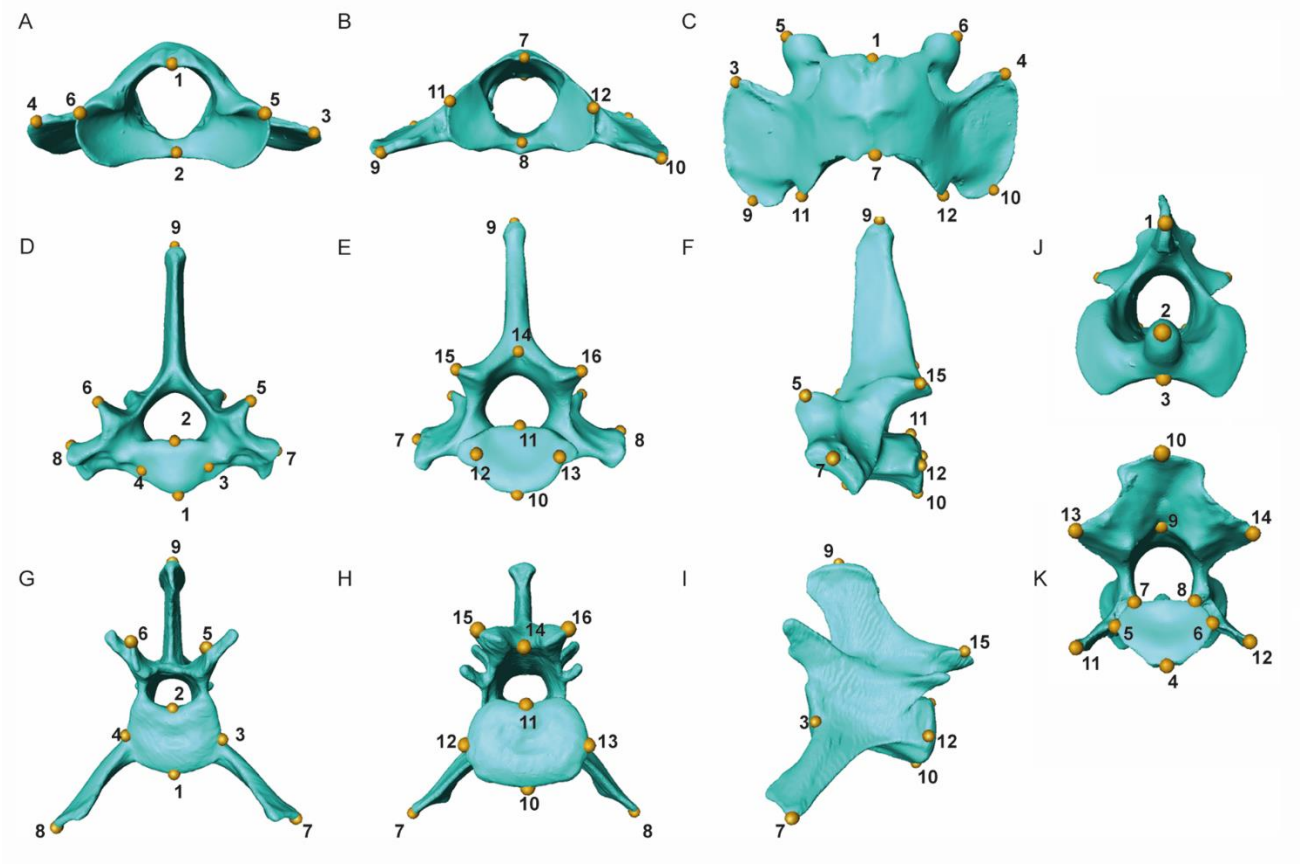

Figure 2: Plots of Principal Component Analyses. (A-B): C4 – L7 PCA plots showing distribution of vertebral elements on PC1xPC2 (A), with respective warps showing extremes of morphology explained by each eigenvector (i.e. PC), and on PC1xPC3 (B). (C): T10 – L7 PCA plot showing distribution of vertebral elements on PC1xPC2, and also displaying eigenvector extremes of vertebral shape. Vertebral types are identified by same colour in all plots (online version), or by labels next to centre of the distribution (printed version)

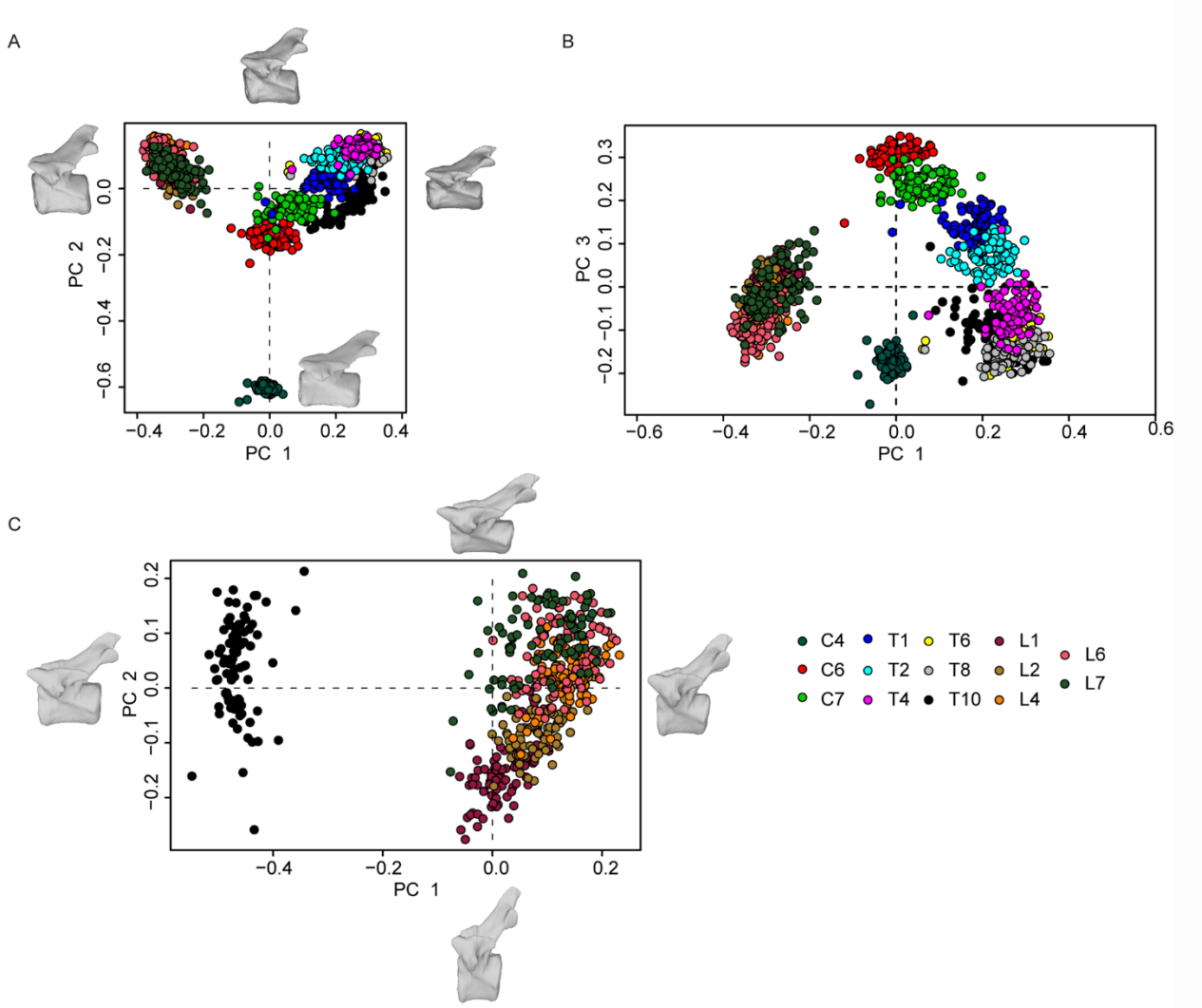

Figure 3: Allometric trajectories displaying the differences in the predicted shape:size relationship between ecological groups. (A): Species groups by their prey size, (B): species grouped by locomotory category.

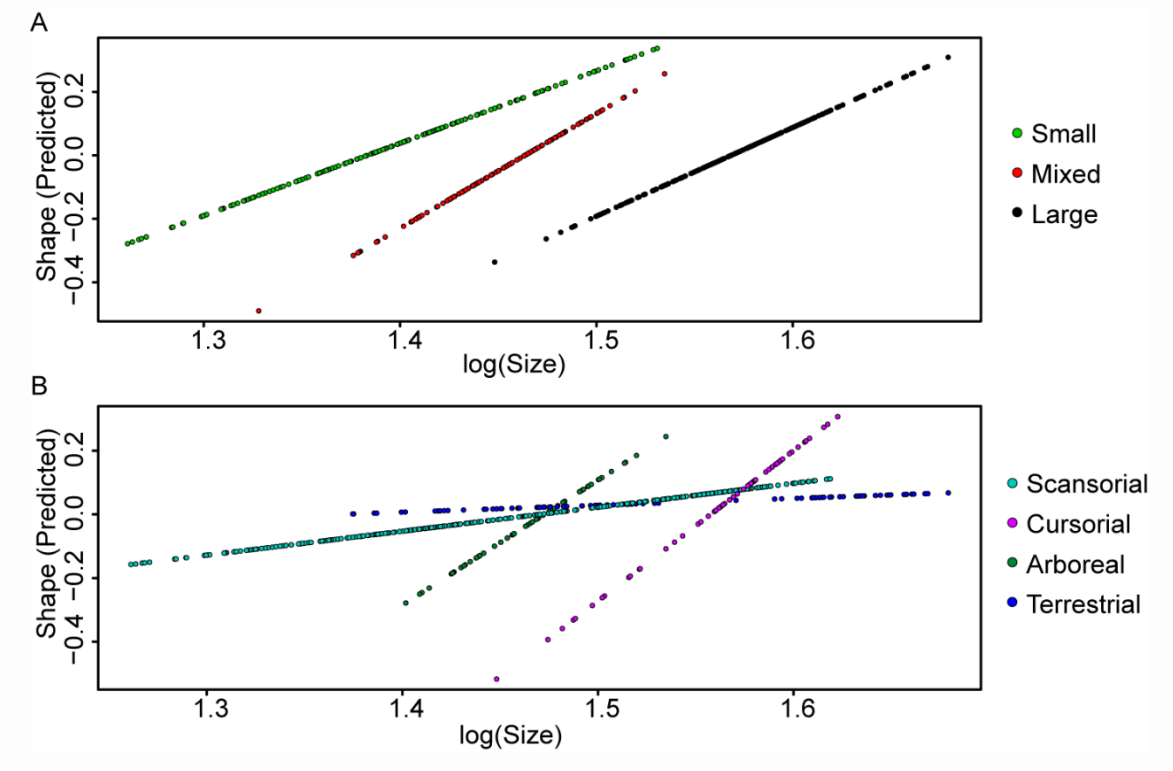

Figure 4: Phenotypic trajectory analysis (PTA) of post-atlantoaxial presacral vertebrae (i.e. C4 – L7) grouped by prey size categories. Larger-sized circles show the average shape location of each individual group per stage. White-filled circles represent the first stage of the trajectory, grey-filled circles represent all intermediate stages, and black-filled circles mark the final stage of each trajectory.

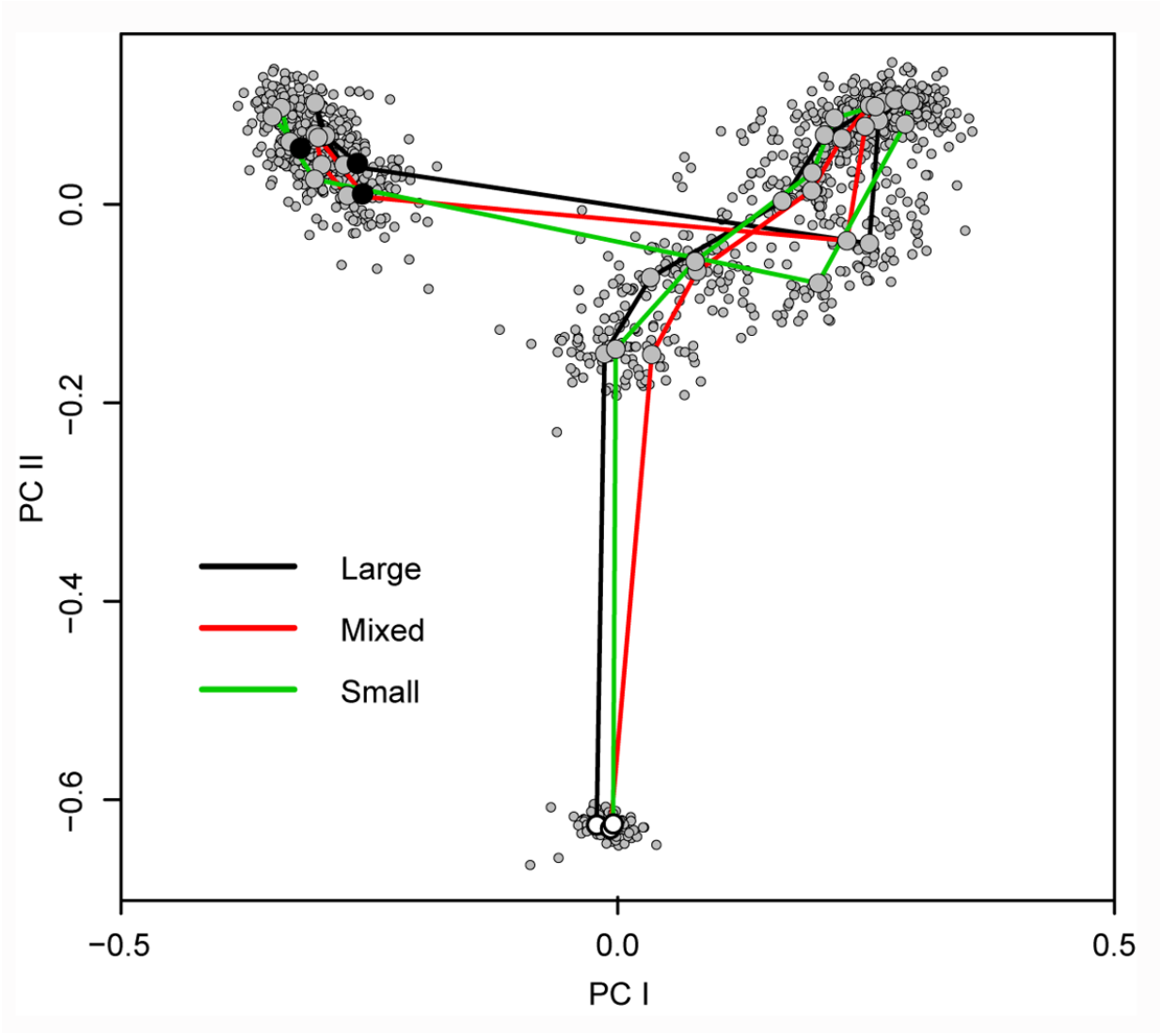

Figure 5: Phenotypic trajectory analysis (PTA) of vertebrae in the T10 – L7 region grouped by prey size (A) and locomotory (B) categories. Larger-sized circles show the average shape location of each individual group per stage. White-filled circles represent the first stage of the trajectory, grey-filled circles represent all intermediate stages, and black-filled circles mark the final stage of each trajectory.

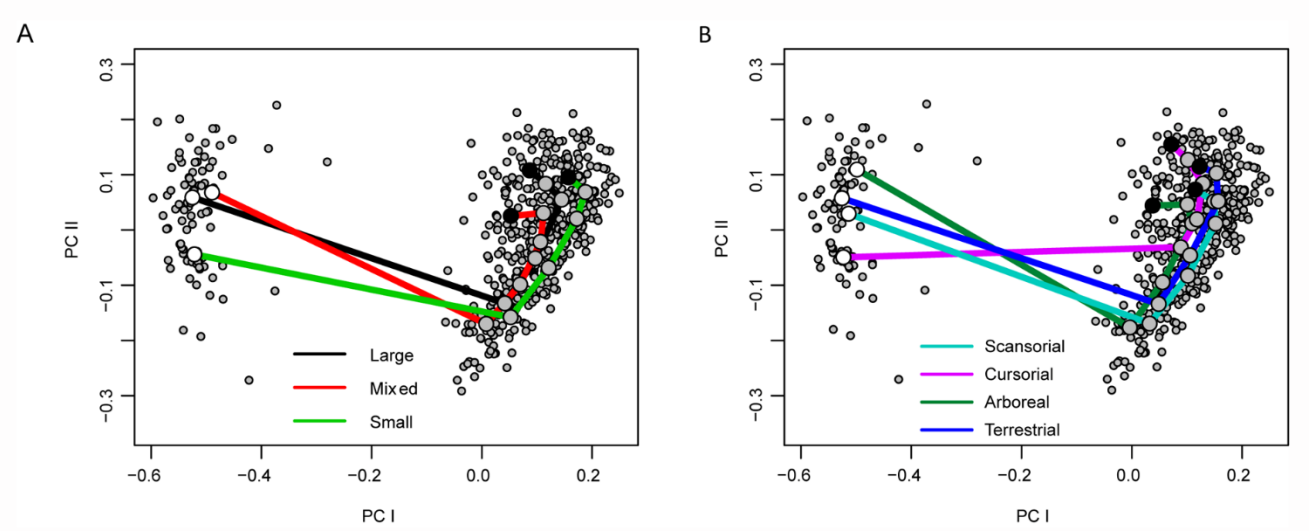

Table 1: PCA C4L7 results

PRINCIPAL COMPONENT	EIGENVALUE	PROPORTION OF VARIANCE	CUMULATIVE PROPORTION
PC1	0.244	0.439	0.439
PC2	0.185	0.251	0.691
PC3	0.142	0.148	0.839
PC4	0.093	0.064	0.903
PC5	0.062	0.028	0.931
PC6	0.041	0.012	0.943
PC7	0.033	0.008	0.951
PC8	0.031	0.007	0.958
PC9	0.025	0.005	0.963
PC10	0.024	0.004	0.967
PC11	0.022	0.004	0.971
PC12	0.020	0.003	0.973
PC13	0.019	0.003	0.976
PC14	0.019	0.003	0.979
PC15	0.018	0.002	0.981
PC16	0.017	0.002	0.983
PC17	0.015	0.002	0.985
PC18	0.014	0.002	0.986
PC19	0.014	0.001	0.988
PC20	0.013	0.001	0.989
PC21	0.012	0.001	0.990
PC22	0.011	0.001	0.991
PC23	0.011	0.001	0.992

PC24	0.010	0.001	0.992
PC25	0.010	0.001	0.993
PC26	0.010	0.001	0.994
PC27	0.009	0.001	0.995
PC28	0.009	0.001	0.995
PC29	0.009	0.001	0.996
PC30	0.008	0.001	0.996
PC31	0.008	0.000	0.997
PC32	0.008	0.000	0.997
PC33	0.007	0.000	0.997
PC34	0.007	0.000	0.998
PC35	0.007	0.000	0.998
PC36	0.007	0.000	0.998
PC37	0.006	0.000	0.999
PC38	0.006	0.000	0.999
PC39	0.006	0.000	0.999
PC40	0.006	0.000	0.999
PC41	0.005	0.000	1.000
PC42	0.005	0.000	1.000
PC43	0.004	0.000	1.000
PC44	0.001	0.000	1.000
PC45	1.20E-16	0.00E+00	1.00E+00
PC46	6.50E-17	0.00E+00	1.00E+00
PC47	5.54E-17	0.00E+00	1.00E+00
PC48	3.94E-17	0.00E+00	1.00E+00

Table 2: PCA T10L7 results

PRINCIPAL COMPONENT	EIGENVALUE	PROPORTION OF VARIANCE	CUMULATIVE PROPORTION
PC1	0.216	0.639	0.639
PC2	0.103	0.145	0.784
PC3	0.065	0.058	0.842
PC4	0.052	0.037	0.879
PC5	0.041	0.023	0.902
PC6	0.035	0.017	0.919
PC7	0.031	0.013	0.932
PC8	0.025	0.009	0.941
PC9	0.025	0.008	0.949
PC10	0.021	0.006	0.955
PC11	0.020	0.005	0.960
PC12	0.018	0.005	0.965
PC13	0.017	0.004	0.969
PC14	0.016	0.003	0.972
PC15	0.015	0.003	0.975
PC16	0.014	0.003	0.978
PC17	0.013	0.002	0.980
PC18	0.012	0.002	0.982
PC19	0.011	0.002	0.984
PC20	0.011	0.002	0.986
PC21	0.010	0.001	0.987
PC22	0.009	0.001	0.988
PC23	0.009	0.001	0.989

PC24	0.009	0.001	0.990
PC25	0.009	0.001	0.991
PC26	0.008	0.001	0.992
PC27	0.008	0.001	0.993
PC28	0.008	0.001	0.994
PC29	0.008	0.001	0.995
PC30	0.007	0.001	0.995
PC31	0.007	0.001	0.996
PC32	0.006	0.001	0.997
PC33	0.006	0.001	0.997
PC34	0.006	0.000	0.998
PC35	0.006	0.000	0.998
PC36	0.006	0.000	0.998
PC37	0.005	0.000	0.999
PC38	0.005	0.000	0.999
PC39	0.005	0.000	0.999
PC40	0.005	0.000	1.000
PC41	0.004	0.000	1.000
PC42	0.000	0.000	1.000
PC43	0.000	0.000	1.000
PC44	0.000	0.000	1.000
PC45	0.000	0.000	1.000
PC46	0.000	0.000	1.000
PC47	0.000	0.000	1.000
PC48	0.000	0.000	1.000

Table 3: Individual vertebral MANOVAs

VERTEBRA	CENTROID SIZE		LOCOMOTION		PREY SIZE	
	P VALUE	R^2	P VALUE	R^2	P VALUE	R^2
atlas	0.001	**0.187**	0.001	*0.074*	0.001	0.080
axis	0.001	0.155	0.001	0.117	0.001	0.081
HOMOLOGOUS DATASET						
C4	0.001	0.080	0.001	0.208	0.001	0.042
C6	0.001	0.083	0.001	0.147	0.007	0.034
C7	0.001	0.089	0.001	0.142	0.003	0.037
T1	0.001	0.083	0.001	0.121	0.001	0.046
T2	0.001	0.063	0.001	0.161	0.001	0.089
T4	0.001	0.095	0.001	0.122	0.001	0.062
T6	0.001	0.099	0.001	0.146	0.001	0.042
T8	0.001	0.059	0.001	0.145	0.062	
T10	0.001	0.183	0.001	0.169	0.016	*0.030*
L1	0.001	0.154	0.001	**0.238**	0.001	0.041
L2	0.001	0.176	0.001	0.185	0.001	0.061
L4	0.001	0.137	0.001	0.130	0.001	0.059
L6	0.001	0.110	0.001	0.105	0.001	0.077
L7	0.006	*0.043*	0.001	0.121	0.001	**0.118**

Table 4: Physignal results

VERTEBRA	MEAN SHAPE	MEAN CENTROID SIZE
	P VALUE	**P VALUE**
ATLAS	**0.002**	0.545
AXIS	**0.002**	0.271
HOMOLOGOUS DATASET		
C4	0.731	0.340
C6	**0.026**	0.405
C7	0.904	0.917
T1	**0.006**	0.373
T2	**0.027**	0.890
T4	0.301	0.370
T6	0.105	0.712
T8	0.221	0.602
T10	0.135	0.149
L1	0.541	0.700
L2	0.056	0.752
L4	0.241	0.445
L6	0.238	0.185
L7	0.124	0.904

Table 5: Phylogenetic MANOVAS in vertebrae

	CENTROID SIZE	LOCOMOTION	PREY SIZE
VERTEBRA	**P VALUE**	**P VALUE**	**P VALUE**
ATLAS	0.23976	0.98501	0.096903
AXIS	0.1968	0.9021	0.14486
C6	0.35265	0.78122	0.071928
T1	0.51149	0.81019	0.064935
T2	0.70529	0.62438	0.26873

Table 6: Regional MANOVAs

	CENTROID SIZE		PREY SIZE		LOCOMOTION	
REGION	**P VALUE**	**R^2**	**P VALUE**	**R^2**	**P VALUE**	**R^2**
C4 - L7	0.001	0.036	0.001	0.070	0.101	
C4 - T10	0.005	0.007	0.001	0.016	0.164	
T1 - T10	0.001	0.023	0.001	0.042	0.002	0.020
T1 - L7	0.001	0.057	0.001	0.126	0.001	0.119
T10 - L7	0.010	0.078	0.010	**0.176**	0.010	**0.122**
L1 - L7	0.001	0.081	0.001	0.109	0.001	0.100

Table 7: Allometric trajectories

	ALLOMETRIC TRAJECTORY	
	SLOPE DISTANCE	SLOPE ANGLE
	P VALUE	P VALUE
LOCOMOTION		
ARBOREAL X CURSORIAL	0.558	0.997
ARBOREAL X SCANSORIAL	**0.002**	0.839
ARBOREAL X TERRESTRIAL	**0.001**	0.212
CURSORIAL X SCANSORIAL	**0.002**	0.864
CURSORIAL X TERRESTRIAL	**0.002**	0.103
SCANSORIAL X TERRESTRIAL	**0.003**	**0.003**
PREY SIZE		
LARGE X MIXED	**0.007**	0.137
LARGE X SMALL	0.107	**0.008**
MIXED X SMALL	**0.002**	0.091

Table 8: C4L7 PTA prey size

	PHENOTYPIC TRAJECTORY		
	SIZE	**DIRECTION**	**SHAPE**
	P VALUE	**P VALUE**	**P VALUE**
PREY SIZE			
LARGE X MIXED	0.639	0.233	**0.001**
LARGE X SMALL	**0.001**	0.123	**0.001**
MIXED X SMALL	**0.001**	0.237	**0.001**

Table 9: T10L7 PTA

	PHENOTYPIC TRAJECTORY		
	SIZE	**DIRECTION**	**SHAPE**
	P VALUE	**P VALUE**	**P VALUE**
LOCOMOTION			
ARBOREAL X CURSORIAL	0.829	**0.001**	**0.012**
ARBOREAL X SCANSORIAL	0.759	**0.001**	0.211
ARBOREAL X TERRESTRIAL	0.933	**0.001**	0.208
CURSORIAL X TERRESTRIAL	0.744	**0.001**	0.180
CURSORIAL X SCANSORIAL	0.890	**0.001**	**0.010**
SCANSORIAL X TERRESTRIAL	0.548	0.144	0.997
PREY SIZE			
LARGE X MIXED	0.203	**0.001**	0.072
LARGE X SMALL	0.955	**0.001**	**0.004**
MIXED X SMALL	0.228	**0.001**	**0.002**